Perovskite Quantum Dots

Subjects: Optics

Contributor: Xinxin Ren, Xiang Zhang, Hongxing Xie, Junhu Cai, Chenhui Wang, Enguo Chen, Sheng Xu, Yun Ye, Jie Sun, Qun Yan, Tailiang Guo

The excellent luminescence properties of perovskite quantum dots (PQDs), including wide excitation wavelength range, adjustable emission wavelength, narrow full width at half maximum (FWHM), and high photoluminescence quantum yield (PLQY), highly match the application requirements in emerging displays.

Keywords: Synthesis Methods ; Fundamental Structure ; Optical Properties ; PQDs

1. Fundamental Structure and Optical Properties of PQDs

1.1. Fundamental Structure of PQDs

Halide perovskites have a general formula of ABX_3, where A and B are, respectively, monovalent and divalent cations, and X is a monovalent halide (Cl, Br, I) anion. The basic structural unit of metal halide perovskites is shown in **Figure 1**d,e, where B-site cations, usually Pb and Sn, will form inorganic octahedra with the six surrounding halide ions. However, when the B site is a mixed cation such as B^{+} and B'^{3+}, the whole structure will form a double-calcite structure with larger crystals. Cubic-phase perovskite (the most regular perovskite) has a corner-sharing structure, which means that the cation at site A is shared by eight neighboring cells, with the location of A at the apex of the cell [1].

The common metal halide perovskites can be further classified into either organic–inorganic (hybrid perovskite quantum dots, HPQDs) or all-inorganic perovskite quantum dots (IPQDs), depending on whether the A cation is an organic molecule such as methylammonium ($CH_3NH_3^+$) and formamidinium (FA^+), or an inorganic cation (commonly Cs^+). The optical and electronic properties of perovskites can be tunable by varying the composition of constituted halide ions and the size of the cations [2][3]. In addition, the dimensionality of perovskites can also be used to tune their optical properties, similar to conventional metal chalcogenide semiconductors [4][5]. Moreover, the reported dimensionality of perovskite can range from the 3D to 0D. Compared with the high-dimensional one, the low-dimensional perovskite nanocrystals (NCs) exhibit very high PLQY partly due to their defect tolerance [3][4][5][6][7][8], high exciton binding energy [9][10][11], high optical absorption coefficient [12][13], and tunable carrier diffusion length [14][15][16].

1.2. Optical Properties of PQDs

After PQDs are excited by external energy, the electrons in the valence band leap into the conduction band, and therefore holes are generated in the valence band. The three types of luminescence are as follows [17]. (1) The electrons return to the valence band and recombine with the holes to emit photons. (2) Electrons are trapped by a defect energy band to emit light. (3) Electrons are trapped by a doped energy level and then emit light.

Four basic optical parameters, including emission stability [18], luminous intensity [18][19][20], color diversity [21][22], and color purity [23], can be used to characterize the luminescence properties of PQDs. It is remarkable that these basic characteristics also determine their application feasibility in display devices. Among them, emission stability is related to the crystal lattice of PQD materials, and luminous intensity is mainly determined by PLQY. Color diversity can be regulated by changing the PQDs' particle size, composition, and type of ionic elements, while color purity is associated with the FWHM of the emission spectrum.

Compared with organic fluorescent dyes and rare-earth-doped phosphors, PQDs show excellent optical properties in the following four aspects: wide excitation wavelength range [18][24], high PLQY [18][19][20], adjustable emission wavelength [21][22], and narrow emission FWHM [23].

(1). Wide excitation wavelength range. The excitation spectra of both organic fluorescent dyes and rare-earth-doped phosphors are relatively narrow and may require the use of excitation sources in specific bands to obtain a desired emission spectrum. By contrast, the excitation spectrum of PQDs is continuous and can be excited by arbitrary light

higher than the bandgap energy. Therefore, the same excitation light source can simultaneously excite PQDs with different band gaps, resulting in different fluorescent colors.

(2). High PLQY. PQDs with a high molar absorption coefficient have excitation overlap regions so that they can absorb large amounts of excitation light for light conversion. In addition, the defect energy levels caused by internal or surface defects in PQDs can be eliminated by optimizing synthesis methods, modified ligands, and coating, so as to obtain high quantum yield by radiation recombination.

(3). Adjustable emission wavelength. Due to the quantum confinement effect [25], the energy band of the semiconductor is split into discrete energy levels, resulting in different sizes of PQDs having different band gaps. In other words, by regulating the particle size, the light-emitting color of PQDs can be easily tuned to the required wavelength range for various applications. Different from other QDs, the luminescence color of PQDs can also be changed by controlling the components of the halogen anions, which has the potential to cover the entire visible spectrum.

(4). Narrow emission FWHM. For PQDs, the relaxation rate of electrons and holes in the band is much higher than the composite rate of thermal excitons. It is hard to have recombination between high-level electrons and holes. Thus, the luminescence spectra of monodispersed PQDs are basically symmetrical. The FWHM is comparable to the low-energy edge of the first exciton absorption peak, and the luminescence peak energy is slightly lower than the first exciton absorption peak.

Based on the above excellent optical properties, PQDs show outstanding performance to better meet the need in emerging display, as shown in **Figure 1**.

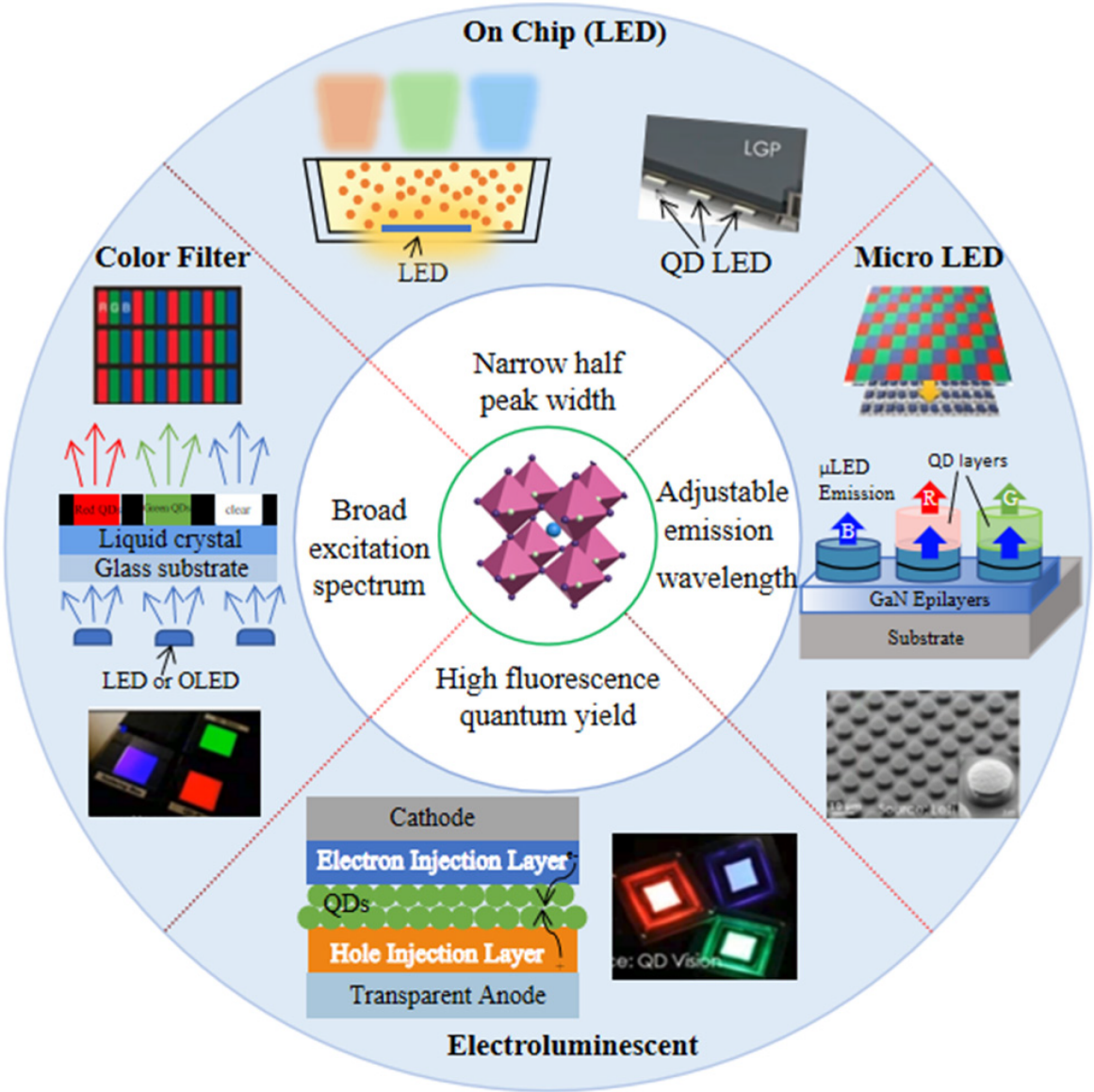

Figure 1. Schematic diagram of the research direction of PQD displays.

2. Synthesis Methods of PQDs

The synthesis of $CsPbX_3$ PQDs showing bright emission and a wide color gamut was first reported by Loredana et al. in 2015, and it is widely known as the hot injection method [26]. The Cs-oleate precursor was prepared in advance, and then injected into a PbX_2 (X = Cl, Br, I) solution dissolved in oleic acid (OA), oleylamine (OAm), and octadecene (ODE) at high temperature and in a nitrogen atmosphere. After a few seconds, the temperature of the reaction system was quickly dropped to room temperature and the PQDs could be obtained via centrifugation. By using this method, the cubic $CsPbX_3$ QDs with a PLQY of 50~90% and an FWHM of 12~42 nm were successfully synthesized, which paved a new way for the development of perovskite. The hot injection method introduces OA, and OAm ligands, providing potential for subsequent studies of ligand modification. In addition, this method facilitates the introduction of ions into perovskite lattice, laying the foundation for the study of ion doping. In the same year, Nedelcu et al. [27] prepared IPQDs by introducing different halogen elements into $CsPbX_3$ QDs for an anion exchange reaction, and finally realized the full spectral luminescence (410~700 nm) with the PLQY of 20~80%.

Due to strict reaction conditions and a complex process, the hot injection method is still difficult for mass production at present. In 2016, the room-temperature reprecipitation method was proposed based on the differences in the solubility of ions in different solvents [28]. OAm and OA as surface ligands and PbX_2 and CsX as ion sources were dissolved in dimethylformamide (DMF) at room temperature to serve as precursors. The precursor at a supersaturated state was injected into the toluene solution and a large number of perovskite crystals were precipitated. The resulting perovskite had excellent optical properties, with a PLQY of 80%, 95%, and 70% and a FWHM of 35 nm, 20 nm, and 18 nm for red, green, and blue, respectively. In this method, ligands function to passivate the QDs' surface to reduce surface defects and inhibit nonradiative recombination to improve the luminescence performance and lifetime. In addition, it is simple to operate without high temperature and an inert gas environment, and it is less affected by the environment. Therefore, it does have high repeatability compared with the hot injection method. In the same year, Tong et al. [29] described a universal nonpolar solvent ultrasound method which mixed precursors of cesium and lead halide with the end-sealing ligand (OAm and OA) in ODE followed by sonication for 10 min. The PLQY of the prepared red, green, and blue perovskites, respectively, reached 90%, 92%, and 10%, and the synthesized $CsPbBr_3$ was highly monodisperse. This simple, fast, and ligand-modifiable method is expected to achieve commercial production of perovskite.

In 2017, the microwave-assisted synthesis of $CsPbX_3$ NCs with different morphologies was first reported by Pan et al. [30]. Cesium acetate, lead halide (PbX_2, X = Cl, Br, I or their mixtures), a certain amount of trioctylphosphine oxide (TOPO), OA, OAm, and ODE were mixed in a microwave quartz tube and then put into a microwave reactor. Nanoplates and nanocubes were obtained at low and high reaction temperature, respectively, while nanorods could be formed by pre-dissolving precursors. This method provided uniform particle size distribution, simple operation, no inert gas, and less environmental impact. Compared with the hot injection method, it has a high repeatability and no other pretreatment. In the same year, the solvothermal method was proposed for the synthesis of IPQDs [31]. Cs_2CO_3 and PbX_2, used as precursors, were mixed with OA, OAm, and ODE in the autoclave and maintained at 160 ℃ for a while. $CsPbX_3$ QDs and ultrathin nanowires with uniform cubic phase were successfully prepared with the PLQY reaching 80%. Although this simple preparation method could obtain high-quality IPQDs with controllable morphology, the uncontrollable system temperature made it rarely used in doping strategies and ligand modification.

The mechanochemical synthesis method was first proposed in 2017 [32]. Solid $PbBr_2$, ABr, and capping ligands were mixed and ground at room temperature for a while. Square and rectangular ($CsPbBr_3$), spherical ($MAPbBr_3$), and parallelogram ($FAPbBr_3$) nanoparticles (NPs) were prepared through this solid-phase method. Although its PLQY of 13% was significantly lower than in traditional liquid-phase method, it still showed certain good characteristics such as high yield, simplicity, and fast synthesis process. Due to the solid reaction system, the ligand modification strategy was hardly applied. For this reason, the wet ball milling method for preparing colloidal nanocrystals was further proposed by Kovalenko et al. in 2018 [33], which was composed of $APbBr_3$ mixed with solvent and oil-based ammonium bromide ligand. In 2019, Palazon et al. [34] revealed the process mechanism, dynamics, and possible side effects of dry ball milling. The changes of mechanochemical synthesis with different time variations were studied in detail, and it was found that the drying and rapid (5 min) process affected the excellent phase purity of IPQDs.

In 2018, Guo et al. [35] synthesized $CsPbX_3$ microcrystals using chemical vapor deposition (CVD) at room temperature. The working process was summarized as follows. PbX_2 and CsX (X = Cl, Br, I) were mixed in a reaction chamber. The substrate could be made of sapphire, SiO_2, or Si. The products $CsPbI_3$, $CsPbBr_3$, and $CsPbCl_3$ were grown at 580 °C, 620 °C, and 620 °C, respectively, with argon at the rate of 100 mL/min and the growth time of 30 min. The fluorescence lifetime was 59.7 ns ($CsPbI_3$), 36.9 ns ($CsPbBr_3$), and 3.5 ns ($CsPbCl_3$), respectively. By using this method, the white-light-emitting chips could be successfully prepared on substrates. Though the large size (μm) and high precision of the

experimental equipment still limit its application, it does show a certain potential in display backlights due to excellent performance of the crystal product.

In recent years, the synthesis of various kinds of nanocrystals with good homogeneity using a fully automated microfluidic platform has become a hot research topic [36][37]. This microfluidic platform allows the parameters of the synthesized nanocrystals to be varied by changing the precursor molar ratio (e.g., Cs/Pb, FA/Pb, Cs/FA, and Br/I), growth time (determined by flow rate and tube length), and temperature in a systematic and independent way. Droplets are generated by adjusting the flow rates of the carrier phase (50~200 μL/min) and that of the dispersed phase (1.2~50 μL/min), and each droplet can be viewed as a small hot-injection reaction system. In 2018, Lignos et al. [37] further explored the synthesis of colloidal QDs in the near infrared using a microfluidic platform. The synthesis results showed that untreated colloidal QDs had an emission FWHM within 45~65 nm. The NCs could further narrow the PL FWHM to 40 nm after a series of post-treatments (e.g., isolation, size selection, and purification), while the synchrotron X-ray scattering clearly showed a cubic structure of $Cs_xFA_{1-x}Pb(Br_{1-y}I_y)_3$ NCs. Finally, the electroluminescent devices prepared by this colloidal QDs obtained a 5.9% EQE.

To sum up, efficient, convenient, and low-cost synthesis methods have been proposed for PQDs, which lay a foundation for its potential applications in displays. **Table 1** summarizes the characteristics, advantages, and disadvantages of the existing perovskite synthesis methods, with references attached.

Table 1. The existing synthesis methods of PQDs.

Methods	Principle	Results	Drawbacks	Reference
Hot injection	**High temperature**	**High yield, good properties, suitable for ion doping and ligand modification, widely used**	**Complex process**	[4]
Anion exchange	**Doping**	**Full-spectrum luminescence, easy X-position doping**	**Multi-step process**	[26]
Room-temperature reprecipitation	**Different solubility**	**Easy operation, high repeatability, suitable for ligand modification**	**Uneven size**	[27]
Ultrasonic method	**Ultrasonic treatment**	**Easy operation, suitable for ligand modification**	**High cost**	[28]
Microwave-assisted synthesis	**Microwave treatment**	**Easy operation, high repeatability, suitable for ligand modification**	**High cost**	[29]
Solvothermal synthesis	**Mixed high temperature**	**Easy to synthesize, controllable morphology**	**System temperature unevenness, not suitable for ion doping and ligand modification**	[30]
Mechanochemical synthesis	**Mixed grinding**	**High yield, easy to synthesize**	**Not applicable to ligand modification**	[31]
Wet ball milling	**Mixed grinding**	**Easy to synthesize**	**Low synthetic efficiency**	[32]
Dry ball milling	**Mixed grinding, solvent-free**	**Fast, high synthetic purity**	**Easy to generate surface defects**	[33]
Chemical vapor deposition	**Chemical reaction, deposition**	**Excellent performance**	**Large size, precise equipment**	[34]
Microfluidic platform	**Carrier spacing reaction**	**Automatic, homogeneity**	**Immature**	[36]

References

1. Abdi-Jalebi, M.; Pazoki, M.; Philippe, B.; Dar, M.I.; Alsari, M.; Sadhanala, A.; Diyitini, G.; Imani, R.; Lilliu, S.; Kullgren, J.; et al. Dedoping of lead halide perovskites incorporating monovalent cations. ACS Nano 2018, 12, 7301–7311.
2. Eperon, G.E.; Stranks, S.D.; Menelaou, C.; Johnston, M.B.; Herz, L.M.; Snaith, H.J. Formamidinium lead trihalide: A br oadly tunable perovskite for efficient planar heterojunction solar cells. Energy Environ. Sci. 2014, 7, 982–988.

3. Zhang, F.; Zhong, H.; Chen, C.; Wu, X.; Hu, X.; Huang, H.; Han, J.; Zou, B.; Dong, Y. Brightly luminescent and color-tunable colloidal CH3NH3PbX3 (X = Br, I, Cl) quantum dots: Potential alternatives for display technology. ACS Nano 2015, 9, 4533–4542.
4. Protesescu, L.; Yakunin, S.; Bodnarchuk, M.I.; Krieg, F.; Caputo, R.; Hendon, C.H.; Yang, R.X.; Walsh, A.; Kovalenko, M.V. Nanocrystals of cesium lead halide perovskites (CsPbX3, X = Cl, Br, and I): Novel optoelectronic materials showing bright emission with wide color gamut. Nano Lett. 2015, 15, 3692–3696.
5. Sichert, J.A.; Tong, Y.; Mutz, N.; Vollmer, M.; Fischer, S.; Milowska, K.Z.; García Cortadella, R.; Nickel, B.; Cardenas-Daw, C.; Stolarczyk, J.K.; et al. Quantum size effect in organometal halide perovskite nanoplatelets. Nano Lett. 2015, 15, 6521–6527.
6. Gonzalez-Carrero, S.; Galian, R.E.; Perez-Prieto, J. Maximizing the emissive properties of CH3NH3PbBr3 perovskite nanoparticles. J. Mater. Chem. A 2015, 3, 9187–9193.
7. Huang, H.; Susha, A.S.; Kershaw, S.V.; Hung, T.F.; Rogach, A.L. Control of emission color of high quantum yield CH3NH3PbBr3 perovskite quantum dots by precipitation temperature. Adv. Sci. 2015, 2, 1500194.
8. Schmidt, L.C.; Pertegas, A.; Gonzalez-Carrero, S.; Malinkiewicz, O.; Agouram, S.; Minguez Espallargas, G.; Bolink, H.J.; Galian, R.E.; Perez-Prieto, J. Nontemplate synthesis of CH3NH3PbBr3 perovskite nanoparticles. J. Am. Chem. Soc. 2014, 136, 850–853.
9. D'Innocenzo, V.; Grancini, G.; Alcocer, M.J.P.; Kandada, A.R.S.; Stranks, S.D.; Lee, M.M.; Lanzani, G.; Snaith, H.J.; Petrozza, A. Excitons versus free charges in organo-lead tri-halide perovskites. Nat. Commun. 2014, 5, 3586.
10. Sun, S.; Salim, T.; Mathews, N.; Duchamp, M.; Boothroyd, C.; Xing, G.; Sum, T.C.; Lam, Y.M. The origin of high efficiency in low-temperature solution-processable bilayer organometal halide hybrid solar cells. Energy Environ. Sci. 2014, 7, 399–407.
11. Manser, J.S.; Christians, J.A.; Kamat, P.V. Intriguing Optoelectronic Properties of Metal Halide Perovskites. Chem. Rev. 2016, 116, 12956–13008.
12. Xing, G.; Mathews, N.; Sun, S.; Lim, S.S.; Lam, Y.M.; Graetzel, M.; Mhaisalkar, S.; Sum, T.C. Long-Range balanced electron- and Hole-Transport lengths in Organic-Inorganic CH3NH3PbI3. Science 2013, 342, 344–347.
13. Motta, C.; El-Mellouhi, F.; Kais, S.; Tabet, N.; Alharbi, F.; Sanvito, S. Revealing the role of organic cations in hybrid halide perovskite CH3NH3PbI3. Nat. Commun. 2015, 6, 7026.
14. Jeon, N.J.; Noh, J.H.; Kim, Y.C.; Yang, W.S.; Ryu, S.; Seok, S.I. Solvent engineering for high-performance inorganic-organic hybrid perovskite solar cells. Nat. Mater. 2014, 13, 897–903.
15. Jiang, Q.; Zhang, L.; Wang, H.; Yang, X.; Meng, J.; Liu, H.; Yin, Z.; Wu, J.; Zhang, X.; You, J. Enhanced electron extraction using SnO2 for high-efficiency planar-structure HC(NH2)2PbI3-based perovskite solar cells. Nat. Energy 2017, 2, 16177.
16. Ponseca, C.S., Jr.; Savenije, T.J.; Abdellah, M.; Zheng, K.; Yartsev, A.; Pascher, T.; Harlang, T.; Chabera, P.; Pullerits, T.; Stepanov, A.; et al. Organometal halide perovskite solar cell materials rationalized: Ultrafast charge generation, high and Microsecond-Long balanced mobilities, and slow recombination. J. Am. Chem. Soc. 2014, 136, 5189–5192.
17. Zhang, D.W. Preparation, Properties and Application of Perovskite Quantum Dots and Metal—Organic Framework Composites; University of Science & Technology Beijing: Beijing, China, 2019.
18. Bai, Y.; Hao, M.; Ding, S.; Chen, P.; Wang, L. Surface Chemistry Engineering of Perovskite Quantum Dots: Strategies, Applications, and Perspectives. Adv. Mater. 2022, 34, 2105958.
19. Byun, J.; Cho, H.; Wolf, C.; Jang, M.; Sadhanala, A.; Friend, R.H.; Yang, H.; Lee, T.-W. Efficient Visible Quasi-2D Perovskite Light-Emitting Diodes. Adv. Mater. 2016, 28, 7515–7520.
20. Bekenstein, Y.; Koscher, B.A.; Eaton, S.W.; Yang, P.; Alivisatos, A.P. Highly Luminescent Colloidal Nanoplates of Perovskite Cesium Lead Halide and Their Oriented Assemblies. J. Am. Chem. Soc. 2015, 137, 16008–16011.
21. Zhou, H.; Yuan, S.; Wang, X.; Xu, T.; Wang, X.; Li, H.; Zheng, W.; Fan, P.; Li, Y.; Sun, L.; et al. Vapor Growth and Tunable Lasing of Band Gap Engineered Cesium Lead Halide Perovskite Micro/Nanorods with Triangular Cross Section. ACS Nano 2017, 11, 1189–1195.
22. Wong, A.B.; Lai, M.; Eaton, S.W.; Yu, Y.; Lin, E.; Dou, L.; Fu, A.; Yang, P. Growth and Anion Exchange Conversion of CH3NH3PbX3 Nanorod Arrays for Light-Emitting Diodes. Nano Lett. 2015, 15, 5519–5524.
23. Zhu, H.; Fu, Y.; Meng, F.; Wu, X.; Gong, Z.; Ding, Q.; Gustafsson, M.V.; Trinh, M.T.; Jin, S.; Zhu, X.Y. Lead halide perovskite nanowire lasers with low lasing thresholds and high quality factors. Nat. Mater. 2015, 14, 636–642.
24. Wang, X.; Bao, Z.; Chang, Y.; Liu, R. Perovskite quantum dots for application in high color gamut backlighting display of Light-Emitting diodes. ACS Energy Lett. 2020, 5, 3374–3396.

25. Alivisatos, A.P. Semiconductor clusters, nanocrystals, and quantum dots. Science 1996, 271, 933–937.
26. Nedelcu, G.; Protesescu, L.; Yakunin, S.; Bodnarchuk, M.I.; Grotevent, M.J.; Kovalenko, M.V. Fast Anion-Exchange in Highly Luminescent Nanocrystals of Cesium Lead Halide Perovskites (CsPbX3, X = Cl, Br, I). Nano Lett. 2015, 15, 5635–5640.
27. Li, X.; Wu, Y.; Zhang, S.; Cai, B.; Gu, Y.; Song, J.; Zeng, H. CsPbX3 Quantum Dots for Lighting and Displays: Room-Temperature Synthesis, Photoluminescence Superiorities, Underlying Origins and White Light-Emitting Diodes. Adv. Funct. Mater. 2016, 26, 2435–2445.
28. Tong, Y.; Bladt, E.; Aygüler, M.F.; Manzi, A.; Milowska, K.Z.; Hintermayr, V.A.; Docampo, P.; Bals, S.; Urban, A.S.; Polavarapu, L.; et al. Highly luminescent cesium lead halide perovskite nanocrystals with tunable composition and thickness by ultrasonication. Angew. Chem. Int. Ed. 2016, 55, 13887–13892.
29. Pan, Q.; Hu, H.; Zou, Y.; Chen, M.; Wu, L.; Yang, D.; Yuan, X.; Fan, J.; Sun, B.; Zhang, Q. Microwave-assisted synthesis of high-quality “all-inorganic” CsPbX3 (X = Cl, Br, I) perovskite nanocrystals and their application in light emitting diodes. J. Mater. Chem. C 2017, 5, 10947–10954.
30. Chen, M.; Zou, Y.; Wu, L.; Pan, Q.; Yang, D.; Hu, H.; Tan, Y.; Zhong, Q.; Xu, Y.; Liu, H.; et al. Solvothermal Synthesis of High-Quality All-Inorganic Cesium Lead Halide Perovskite Nanocrystals: From Nanocube to Ultrathin Nanowire. Adv. Funct. Mater. 2017, 27, 1701121.
31. Jana, A.; Mittal, M.; Singla, A.; Sapra, S. Solvent-free, mechanochemical syntheses of bulk trihalide perovskites and their nanoparticles. Chem. Commun. 2017, 53, 3046–3049.
32. Protesescu, L.; Yakunin, S.; Nazarenko, O.; Dirin, D.N.; Kovalenko, M.V. Low-Cost Synthesis of Highly Luminescent Colloidal Lead Halide Perovskite Nanocrystals by Wet Ball Milling. ACS Appl. Nano Mater. 2018, 1, 1300–1308.
33. Palazon, F.; El Ajjouri, Y.; Sebastia-Luna, P.; Lauciello, S.; Manna, L.; Bolink, H.J. Mechanochemical synthesis of inorganic halide perovskites: Evolution of phase-purity, morphology, and photoluminescence. J. Mater. Chem. C 2019, 7, 11406–11410.
34. Guo, P.; Hossain, M.K.; Shen, X.; Sun, H.; Yang, W.; Liu, C.; Ho, C.Y.; Kwok, C.K.; Tsang, S.; Luo, Y.; et al. Room-temperature red-green-blue whispering-gallery mode lasing and white-light emission from cesium lead halide perovskite (CsPbX3, X = Cl, Br, I) microstructures. Adv. Opt. Mater. 2018, 6, 1700993.
35. Lignos, I.; Maceiczyk, R.; de Mello, A.J. Microfluidic Technology: Uncovering the Mechanisms of Nanocrystal Nucleation and Growth. Acc. Chem. Res. 2017, 50, 1248–1257.
36. Lignos, I.; Morad, V.; Shynkarenko, Y.; Bernasconi, C.; Maceiczyk, R.M.; Protesescu, L.; Bertolotti, F.; Kumar, S.; Ochsenbein, S.T.; Masciocchi, N.; et al. Exploration of Near-Infrared-Emissive Colloidal Multinary Lead Halide Perovskite Nanocrystals Using an Automated Microfluidic Platform. ACS Nano 2018, 12, 5504–5517.
37. Li, X.; Cao, F.; Yu, D.; Chen, J.; Sun, Z.; Shen, Y.; Zhu, Y.; Wang, L.; Wei, Y.; Wu, Y.; et al. All inorganic halide perovskites nanosystem: Synthesis, structural features, optical properties and optoelectronic applications. Small 2017, 13, 1603996.